Multielectron dynamics in complex ions irradiated by short laser pulses

Contact m.lysaght@qub.ac.uk

M. A. Lysaght, L. Hamonou, S. Hutchinson, P. G. Burke and H. W. van der Hart

Centre for Theoretical Atomic, Molecular and Optical Physics, Queen's University Belfast, Belfast BT7 1NN, UK

Introduction

At present, most numerical simulations for multi-electron atoms irradiated by ultra-short light fields employ the single-active-electron (SAE) approximation [1], in which only one electron is assumed to be 'active'. To properly describe the response of complex atoms to ultra-short pulses, however, approaches need to accurately describe both multi-electron atomic structure and the multi-electron response to the few-cycle light field. We have therefore developed time-dependent *R*-matrix (TDRM) theory to describe complex atoms and ions in intense ultra-short light pulses [2,3]. In this report we use both the full TDRM method and a restricted inner region version (TDRMI) [4] to investigate complex ions irradiated by intense short laser pulses.

Time-dependent R-matrix theory

In TDRM theory, the time-dependent Schrödinger equation (TDSE) is solved by partitioning configuration space into an inner and an outer region with the boundary at radius $r = a_0$ (see figure 1). In the inner region, electron exchange and correlation effects between the ejected electron and the remaining electrons are important. In the outer region, exchange is negligible, and the ejected electron moves in the local long-range potential of the residual atom together with the laser potential.

In the inner region, an *R*-matrix basis expansion of the wave function is adopted and we use the recently developed TDRMI approach [4] to set up a system of linear equations. Using a linear solver at each time step, we can calculate the *R*-matrix, **R**, on the boundary, $r = a_0$, of this region and also calculate an inhomogeneous *T*-vector, **T**, both as defined in [3].

In the outer region $a_0 \le r \le a_p$, a set of coupled differential equations describing the motion of the scattered electron in the presence of the light field is solved at each time-step by sub-dividing this region into *p* sub-regions and propagating the *R*-matrix and *T*-vector across them from $r = a_0$ to $r = a_p$ as shown in figure 1. The *R*-matrix and *T*-vector at $r = a_p$ can be used to propagate the wave function (*F* in figure 1) backwards across the *p*-sub-regions. This propagated wave function then provides the starting point for the calculation at the next time-step.

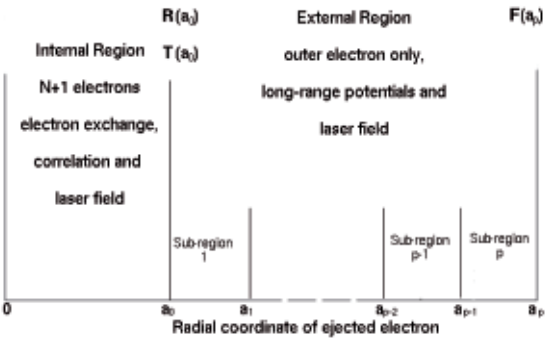

Figure 1. Partitioning of configuration space in TDRM theory.

Investigations of collective electron dynamics in C^+

One of the outstanding questions in atomic physics on the ultra-short timescale is how electron-electron correlation affects the electron dynamics of atomic systems and how such collective dynamics can be observed. We thus propose an ultra-fast pump-probe experiment in which collective dynamics driven by the dielectronic repulsion in excited states of C^+ can be extracted.

We consider C^+ in its $1s^2 2s^2 2p\ ^2P^o$ ground state with total magnetic quantum number M=0. This ion is excited by an ultra-short linearly polarized pulse into a superposition of the $2s^2 2p\ ^2S^e$ and $^2D^e$ states as shown in figure 2. The energy separation between the $2s^2 2p$

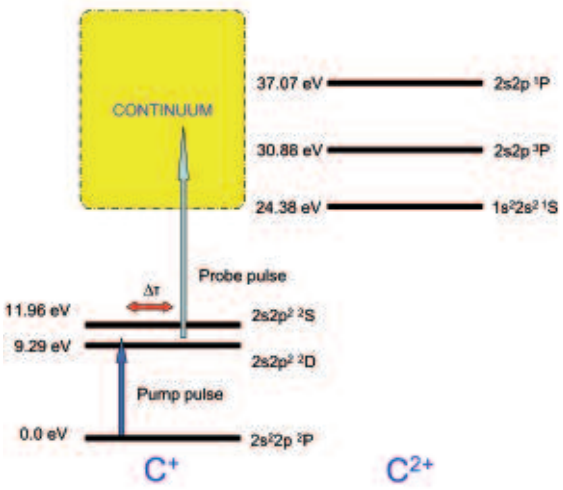

Figure 2. The pump-probe scheme.

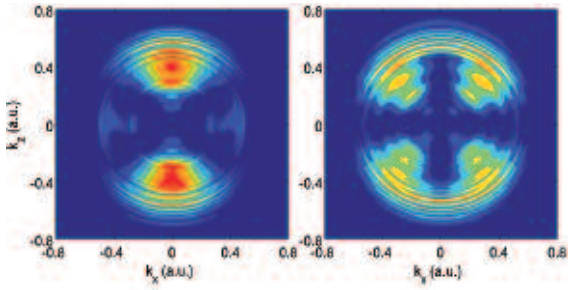

Figure 3. 2D momentum distributions of the ejected electron. Left (a) is for a time delay of 4.16 fs and right (b) is for a delay of 4.89 fs.

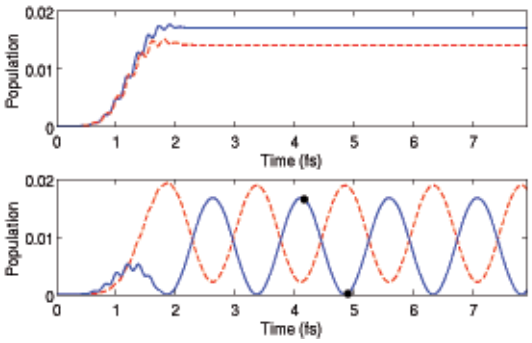

Figure 4. Population of the excited states as a function of time. Top: the ^2S population is shown in blue and the ^2D population is shown as red dashes. Bottom: Both the $|2p_0, 2p_0>$ population (blue solid line) and the $|2p_1, 2p_{-1}>_S$ population (red dashes). The filled circles indicate the two time delays at which the system was probed.

$^2S^e$ and $^2D^e$ states, caused by the Coulomb repulsion between the two equivalent 2p electrons, results in a temporal interference between the two states with a frequency determined by the energy separation. Naïvely, the responsible dielectronic repulsion integral is the F^2 (2p, 2p) integral. Hence, this repulsion governs the dynamical behaviour of the electronic wavepacket (EWP), which continues to evolve after the end of the pump pulse. Subsequent irradiation of the C^+ ion with a time-delayed XUV ultra-short pulse will ionise the ion.

In our current study we use a probe pulse with a central photon energy ω_2 = 21.8 eV, which provides enough energy to transfer the population from the $2s2p^2\ ^2S^e$ and $^2D^e$ excited states to continuum channels coupled to the $2s2p\ ^3P^o$ first excited state of C^{2+}. This means that the outgoing electron has the possibility of having m = -1, 0, or 1 which allows us to investigate the collective dynamics by observing the angular distribution of the ejected electron, as shall be seen below.

Results

Figure 3 shows the 2D momentum spectra of the ejected electron in the k_xk_z plane for two different time delays between the pump pulse and probe pulse. The momentum spectra are obtained by transforming the continuum wave functions coupled to the $2s2p\ ^3P^o$ excited state of C^{2+} at the end of the calculation into the momentum representation.

Figure 3(a) shows that, at a delay of Δt = 4.16 fs, the angular distribution of the ejected electron is aligned predominantly along the laser polarization axis indicating the ejection of an m=0 electron. However, figure 3(b) shows that, at a longer time delay of 4.89 fs, the angular distribution of the ejected electron exhibits the behaviour of an electron with $|m|$ = 1.

To understand this behaviour, we start by investigating the populations of the "probed" $2s2p^2\ ^2S^e$ and $^2D^e$ excited states inside the C^+ ion as a function of time. The top half of figure 4 shows the population of the $2s2p^2\ ^2S^e$ and $^2D^e$ excited states as a function of time, where t = 0 is the start time of the pump pulse. The behaviour of the bound-state population shows no sign of any interference effect which could give rise to the behaviour of the angular distributions of the emitted electron seen in figure 3.

We can explain the dynamics by transforming[5] from the LS-coupled basis to the uncoupled $|2p_m2p_{-m}>$ basis, in which the role of magnetic substates becomes transparent. The bottom half of figure 4 shows the population of $|2p_m2p_{-m}>$ over time, which explains the observed angular distributions. After C^+ has been excited by the pump pulse, the excited multi-electron wavepacket is in a breathing motion between two $|2p_m2p_{-m}>$ states. When the population of $|2p_0,2p_0>$ has reached a maximum, the probe pulse interacts with a state dominated by m=0 electrons, and hence the angular distribution of the ejected electron will be aligned along the laser-polarization axis (figure 3(a)). When the population of $|2p_1,2p_{-1}>_S$ has reached a maximum, the probe pulse interacts with a state dominated by $|m|$=1 electrons, yielding an angular distribution of the outgoing electron directed at an angle to the laser polarization axis (figure 3(b)). The present pump-probe scheme thus allows the observation of collective breathing motions in superpositions of low-lying atomic states. The frequency of these motions is a measure of the magnitude of electron-electron repulsion.

Inner-shell processes in two photon ionisation of Ne^+

We have also applied the TDRMI approach[4] to investigate two-photon ionization of Ne^+, following experimental studies of sequential double ionization of Ne[6]. We have demonstrated recently that the two-photon ionization rates of Ne^+ near the experimental photon energy of 38.4 eV are enhanced by an order of magnitude due to inner-shell processes[7]. Application of the TDRMI approach to this problem provides further insight into the physics of this process. The R-matrix Floquet (RMF) approach is well suited for elucidating the atomic-structure effects on the ionization rates. To study the influence of the pulse shape, however, a time-dependent approach is needed.

Figure 5 shows the ionization probability of Ne^+ irradiated by laser pulses with a photon energy of 38.4 eV and peak intensity of 10^{14} Wcm^{-2}. The pulse shape is a three-cycle $\sin^2$ turn-on, followed by C cycles at constant intensity, and a three-cycle turn-off. Overall, the ionization probability increases linearly with pulse length for C>6. This increase corresponds to the expected ionization rate from RMF calculations. Figure 5 shows oscillations, which are due to excitation

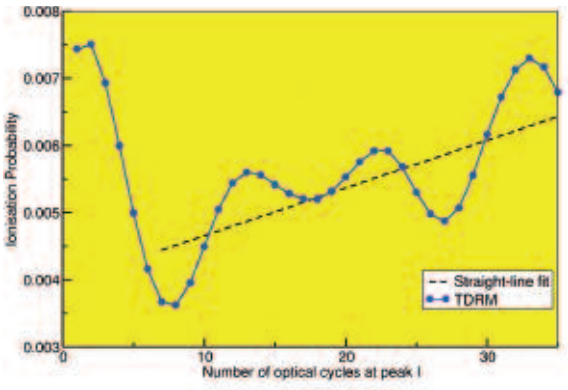

Figure 5. Ionization probability of Ne^+ as a function of number of cycles at peak intensity of 10^{14} W cm^{-2} for a photon energy of 38.4 eV. The laser field is turned on and off by a 3-cycle sin^2 profile.

of autoionizing states just above the $2s^22p^4\ ^3P^e$ Ne^{2+} threshold: Rydberg states converging to the $2s^22p^4\ ^1D^e$ and $^1S^e$ thresholds. The fit gives a large ionization probability at C=0, which is due to the turn-on and turn-off of the laser. These introduce additional frequency components, which allow direct single-photon ionization.

Conclusions

We have developed a time-dependent R-matrix approach for the study of ultra-fast ionization processes. Ultra-fast excitation of an isolated configuration leads to ultra-fast dynamics within the configuration, driven by dielectronic repulsion. The dynamics can be visualized by ultra-fast photoionization in the angular distribution of the emitted electron. Studies of the same ionization process by the TDRM approach and the time-independent RMF approach allows detailed investigations of the involved physics, verifying the importance of specific atomic structure, as well as the influence of short-pulse effects.

Acknowledgements

MAL was supported by Grant No. EP/E000223/1 from the UK Engineering and Physical Sciences Research Council, SH by the Department of Employment and Learning NI under the Programme for Government, and LH by the European Social Fund under its Building Sustainable Prosperity Programme.

References

1. M. Abu-samha *et al.*, *J. Phys. B* **41**, 151001 (2008).
2. M. A. Lysaght *et al.*, *Phys. Rev. Lett*. **101**, 253001 (2008).
3. M. A. Lysaght *et al.*, *Phys. Rev. A* **79**, 053411 (2009).
4. H. W. van der Hart *et al.*, *Phys. Rev. A*, **76**, 043405 (2007).
5. M. A. Lysaght *et al.*, *Phys. Rev. Lett*. **102**, 193001 (2009).
6. A. A. Sorokin *et al.*, *Phys. Rev. A* **75**, 051402 (2007).
7. L. Hamonou *et al.*, *J. Phys. B* **41**, 121001 (2008).